The Impact of Future Urban Scenarios on a Severe Weather Case in the Metropolitan Area of São Paulo

Andréia Bender • Edmilson Dias Freitas • Luiz Augusto Toledo Machado

Received: DD Month YEAR/ Accepted: DD Month YEAR

Abstract In this work, convective parameters are applied, based on numerical simulations made with BRAMS model, to a severe weather case occurred in the Metropolitan Area of São Paulo (MASP). Scenarios of future urban area growth and increase of building heights were made to evaluate changes in convective parameters, rainfall, and in severe weather occurrence probability for the study region. Using factorial planning and factor separation methods, we found that the urban area growth predicted for 2030 is capable of increasing the amount of precipitation, mainly due to the land use change from rural to urban. In the scenario of building heights increasing, it was found a tendency for rainfall suppress. The urban area for 2030 is the major factor contributing to increase atmospheric instability when compared to other experiments. Also, we observed an increase in wind shear and consequently, a higher potential for severe weather occurrence. Vertical urban growing also causes an increase in atmospheric instability, but a decrease in wind shear. The interaction between urban area and building height factors show an increase in the area with precipitation and severe weather probability, nevertheless, weaker and dislocated to south than could be in an urban soil with low buildings.

Keywords Convective Parameters • Severe weather • Urban heat island

---

Andréia Bender • Edmilson Dias Freitas
Departamento de Ciências Atmosféricas, Instituto de Astronomia, Geofísica e Ciências Atmosféricas, Universidade de São Paulo, São Paulo, 05508-090, Brasil.
e-mail: andreia.bender@gmail.com
Edmilson Dias Freitas
e-mail: edmilson.freitas@iag.usp.br
Luiz Augusto Toledo Machado
Centro de Previsão de Tempo e Estudos Climáticos, Instituto Nacional de Pesquisas Espaciais
Rodovia Presidente Dutra, km 40, Cachoeira Paulista, São Paulo, 12630-000, Brasil
e-mail: luiz.machado@inpe.br

1 Introduction

The Metropolitan Area of São Paulo (MASP) is under risk of intense weather events every rainy season, which has as consequences strong winds, heavy precipitation and hail. These events are responsible for tree falls, damaging houses, storages and vehicles, for flooding and landslides (the last related to high accumulated precipitation). Therefore, these phenomena can cost several material losses and even human lives [*E D Freitas et al.*, 2009a]. According to Haddad and Teixeira [2015], in 2008, 749 flood points were identified in the city of São Paulo and the direct loss in a conservative scenario was calculated to be around US 14.0 million dollars for the city. Due to the indirect effects within the long chain of production and income, the loss reaches more than US 72 million dollars to the Brazilian economy.

Following the definitions of Johns and Doswell [1992] and Moller [2001], severe weather is any type of storm capable of generating at least one of these phenomena: tornado, strong surface winds, reaching speeds faster than 94 km h^{-1}, or hail diameter larger than 1,9 cm. Mills and Conquhoun [1998], in a quite similar way, define severe weather as a storm capable of generating at least one of these phenomena: tornado, strong surface winds, reaching speeds higher than 90 km h^{-1}, hail diameter larger than 2 cm or high precipitation rates, sufficient to cause floods. In the case of the Metropolitan area of São Paulo, a vulnerable area, most of intense weather cases have consequences similar to severe weather event, these are cases related to high amounts of precipitation and strong winds, being tornado occurrence observed only in the neighborhood. Other intense-weather characteristic at MASP is the occurrence of lightning, which can interrupt energy distribution and have consequences in several sectors of society [*Morales et al.*, 2010]. Nascimento [2004] used atmospheric soundings and numerical model profiles to verify some convective-parameter skills to indicate severe weather conducing conditions, called proximity soundings [*Brooks et al.*, 1994]. His results suggest promising utility for convective parameters in southern Brazil, although their thresholds were based on middle latitudes systems.

According to theoretical models, different kind of storms (isolated or organized) can have distinct vertical structure and internal dynamic [*Cotton and Anthes*, 1992]. Also, the severe weather forecast is complex because of the different scales related, in time and space. Some synoptic conditions show developments from the microscale to the mesoscale. Cotton and Pielke [1995] verified that Urban Heat Island (UHI) effect is a factor that contributes to storm initiation, which usually adds to the effects of storm generator systems, causing to the storms a higher degree of severity.

Silva Dias et al. [2013] indicate that UHI can interact with sea breeze and mountain-valley circulations that arrive at the MASP by its southeastern portion, being some of the factors responsible for precipitation extremes in the region. Climatic features, indicated by climatic indexes, and local sea surface temperature, which explain a smaller fraction of these events during the rainy season in comparison with the dry season, are other factors found by the authors. The authors also suggest that UHI increasing and the role of air pollution need to be taken into account to explain the observed trends in the increase of higher precipitation amounts over the last eight decades analyzed in their study. The UHI creates a strong convergence zone in a large portion of the MASP, and then, accelerates the breeze front propagation toward the city center [*E D Freitas et al.*, 2007]. In the work of Freitas et al. [2007], the interaction between sea breeze and UHI circulation was reproduced using the mesoscale model BRAMS [*S R Freitas et al.*, 2005] coupled with the Town Energy Budget scheme – TEB [*Masson*, 2000]. With a similar approach, Souza et al. [2016] studied Manaus urban evolution and verify that the growth of urban area has direct relationship with the rising of precipitation intensity and amount.

Freitas et al. [2009a] suggest that, besides sea breeze and UHI, other kind of local circulation, such as those generated by topography, also can have contribution to the storms initiation. Rojas et al. [2018] used the Advanced Regional Prediction System, ARPS [*Xue et al.*, 2000], coupled with the Tropical Town Energy Budget scheme, tTEB [*Karam et al.*, 2010], to simulate the interaction among sea breeze, mountain-valley and UHI circulation over MASP. They found that topography channels and directs the surface acceleration vectors towards the MASP, which can intensify surface winds and its interactions with other mesoscale features, contributing for development of severe weather.

Aerosol it is an important component of urban atmosphere due to the large emissions of pollution in the cities, which can lead to an increase in cloud condensation nuclei, as mentioned by Kusaka et al [2014], and then decrease the mean droplet radius, inhibiting precipitation [*Kaufmann et al.*, 2007; *Rosenfeld*, 2000]. On the other hand, there is the hypothesis of convective invigoration, van der Heever and Cotton [2007], using a three-dimensional model with bulk microphysics, argument that urban aerosol can enhance convective precipitation. Similar results were obtained by Han et al. [2012], which showed that aerosol intensify deep convection but delays initiation of precipitation. Although aerosol importance, our focus in this paper will really on soil use impact on instability associated with UHI.

A future urban area for 2030, predicted by Young [2013], motivated the question about storm severity increase in an even larger urban area. Besides the urban area growth, which can be a factor for more severity in the storms in the region, as shown by Silva Dias et al. [2013], other acceptable hypothesis for future urban modification is the vertical rising of a preexistent urban area, i. e. the change from small houses to higher residential buildings. The current land use master plan and zoning ordinances of São Paulo city motivate this hypothesis. This master plan allows construction of high buildings in areas currently occupied by houses in residential areas. Therefore, the goal of this paper is to verify the impact of different future land use scenarios on severe weather systems in the MAPS, which can be used to generate discussions about city growth.

Section 2 presents the experiments sets. Section 3 shows a storm case study and a control experiment. Section 4 discusses sensitivity experiments with future scenarios of urban growth and section 5 presents our conclusions.

2 Model Experiments

The Brazilian developments on the Regional Atmospheric Modeling System – BRAMS – version 5.0 [*S R Freitas et al.*, 2009b] was used to simulate all experiments. The model is coupled with the Town Energy Budget – TEB – scheme [*Masson*, 2000], which is triggered when an urban type grid cell is present on a patch of land use data. This urban parametrization aims to simulate turbulent fluxes as well as dynamic and thermodynamic interactions between the cities and the atmosphere.

Land use data from U. S. Geological Survey (USGS) is used, although it was modified in some experiments. Young [2013] generated an urban expansion model for MASP until the year of 2030 in order to access environmental risk for the future. The expansion model was generated from an interpolation from satellite imagery, considering a constant annual urban growth rate and taking the pattern of land use observed between 2001 and 2008. This growth rate was applied to the algorithm: $P(t) = P_0(1+i)t$; where, P_0 is Initial Urbanization; $P(t)$ is growth after t years; i is unitary growth rate and t is time in years. Appling this algorithm with an annual growth rate and the number of years, one can project in the future. Thus, it was possible to obtain an urban area for 2030. Fig 1 extrapolates this prediction for all MASP limits, which will be used as one of our land use future scenarios.

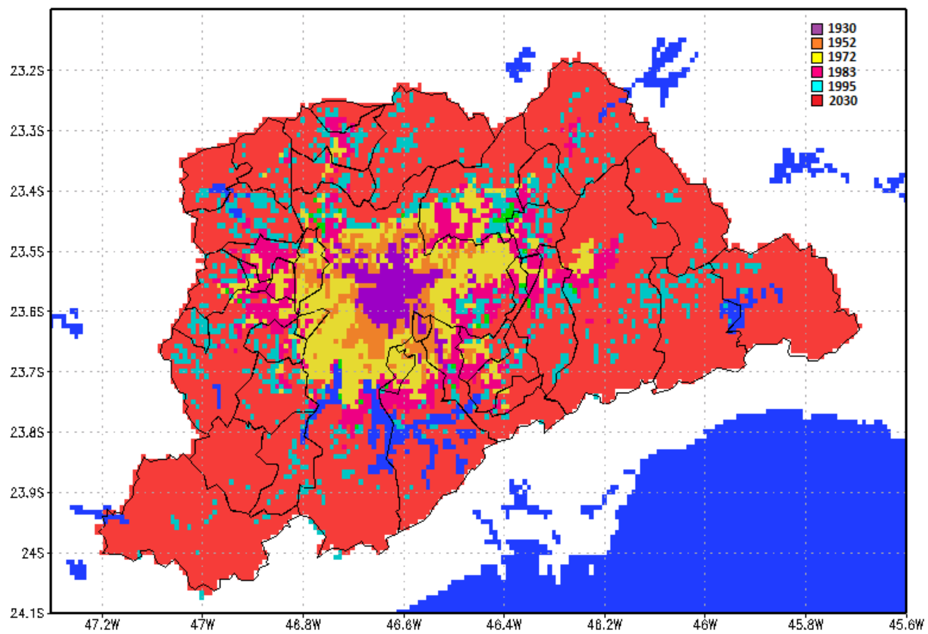

Fig 1 Evolution of urbanization in MASP (historical survey until 1972 by Villaça (1978), for 1983 and 1995 the area may be found in CESAD (http://www.cesadweb.fau.usp.br/index.php)). Red is the extrapolation of the predicted urban area for 2030, adapted from Young (2013).

To identify the effect of urban area expansion for 2030 and the effect of a future vertical expansion on storms, we made experiments based on Factorial Planning [*Barros Neto et al.*, 1995] or Factor Separation [*Stein and Alpert*, 1993] method. This method allows obtaining individual contributions of each parameter in the simulation/forecast of a meteorological variable. In this work, for sensitivity experiments we use two parameters, namely horizontal and vertical urbanization, thus, it is necessary to conduct four simulations (since the number of experiments is equal to 2^n, where n is the number of factors). Table 1 shows sets for the experiments. Experiment 1 is further called control experiment.

Table 1 Factor Separation Experiments (Plus and minus symbols means the factor is included or excluded, respectively).

Experiment	Horizontal Urbanization	Vertical Urbanization	Precipitation-Accumulated
1	Current Area (-)	Current building height (-)	P1
2	2030’s Area (+)	Current building height (-)	P2
3	Current Area (-)	Future building height (+)	P3
4	2030’s Area (+)	Future building height (+)	P4

The current and 2030’s areas are composed with two urban types; the central area, composed by high rising buildings (Urban 1) and its surrounding composed by houses and low commercial buildings (Urban 2). Table 2 and Table 3 show the parameters of urban areas over MASP for experiments with current and future building height.

Table 2 Average parameters of urban areas for Experiments 1 and 2 (with current building height)

Parameter	Urban 1	Urban 2
Building height (m)	50	5
Roughness length (m)	3	0.5
Fraction occupied by buildings	0.5	0.7

Table 3 Average parameters of urban areas for Experiments 3 and 4 (with future building height)

Parameter	Urban 1	Urban 2
Building height (m)	50	50
Roughness length (m)	3	3
Fraction occupied by buildings	0.5	0.5

The fraction occupied by buildings is defined as the average fractional area occupied by buildings in the grid cell. The roughness length was defined according to Grimmond and Oke [1999], which suggest roughness lengths ≥ 2 m for high-rise urban surfaces (building heights ≥ 20 m) and according to Masson [2000], which mentioned a review of experimental estimations of Wieringa [1993], where roughness length are approximately equal to 1/10 of the house or building heights.

According to Barros Neto et al. [1995], the main effect of urban expansion over precipitation is, by definition, the average of Urban Area Effects (UAE) in two levels of high-buildings area, given by:

$$UAE = \frac{1}{2}[(P2 - P1) + (P4 - P3)] \ , \tag{1}$$

where UAE is the effect of urban area growth and P1, P2, P3 and P4 are accumulated precipitation for experiments 1, 2, 3 and 4, respectively. Similarly, the effect of High-Buildings Area Expansion (HBAE) over precipitation is given by the average high-buildings area effect in two levels of urban area, given by:

$$HBAE = \frac{1}{2}[(P3 + P4) - (P1 + P2)] \ , \tag{2}$$

where HBAE is the effect of high-buildings area growth. The interaction between both parameters, UAE_HBAE, is given by:

$$UAE\_HBAE = \frac{1}{2}[(P1 + P4) - (P2 + P3)] \ , \tag{3}$$

Stein and Alpert (1993) defined UAE and HBAE in a different way as the simply difference between a variable with the factor and other from control experiment (without the factor):

$$UAE = \mathrm{P2} - \mathrm{P1} \tag{4}$$

$$HBAE = \mathrm{P3} - \mathrm{P1} \tag{5}$$

The interaction between two factors, UAE_HBAE, is given by:

$$\mathrm{UAE\_HBAE} = \mathrm{P4} - (P2 + P3) + P1 \tag{6}$$

The storm case simulation was started at 00 UTC on February 14th, 2013 for a 24 hours integration period. Three nested grids with 16, 4 and 1 km of horizontal grid spacing, in a domain made with 150x150, 202x202 and 270x270 points, respectively, centered at 23ºS and 46ºW were used for the simulations. The grids location is given in Fig 2. In the vertical we applied 35 sigma-z type points, initially spaced by 50 m with an increasing factor of 1.2, until 1000 m, keeping this vertical grid spacing until the top of model domain. Global Forecast System (GFS) analysis with 0.5º of resolution were used as initial and boundary conditions. Shortwave and longwave radiation were treated accord with Chen and Cotton [1983] parameterization. Grell Ensemble [*Grell and Devenyi*, 2002] formulation was used as cumulus parametrization while 3 levels of moisture complexity [*Meyers et al.*, 1997; *Walko et al.*, 1995] was applied to parametrize microphysical process. Eddy diffusion parametrization was based on Mellor and Yamada [1982].

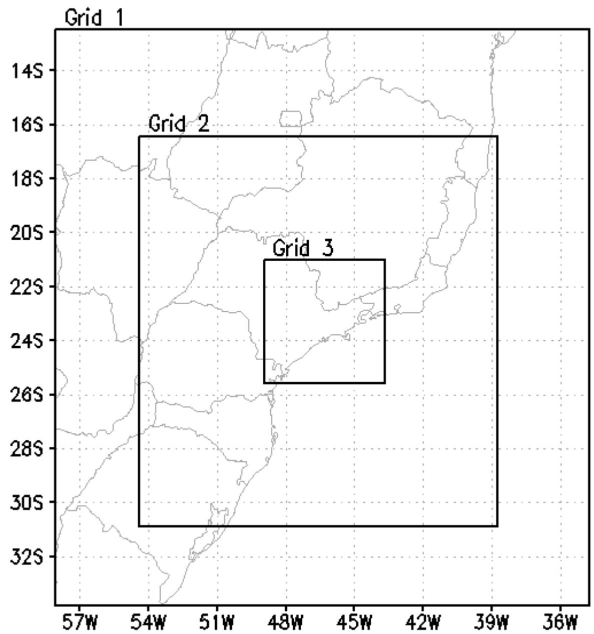

Fig 2 Experiments grid location.

3 Storm Case Study and Control Experiment

The storm happened in São Paulo, on February 14th, 2013, draws our attention because its explosive convection when arrived at MASP, which suggests the UHI and the urban area effect. This Fig. shows the system crossing different land uses, changing from rural to urban, with different types of urban structures, from low to high rising buildings. Carraça and Collier [2007] studying a convective case in Manchester observed that a convective cell was initiated by the sensible heat flux generated by the high-rise buildings in the Manchester center. Fig 3 shows radar reflectivity for the storm and its evolution. At 18:45 GMT convection starts on the borders of São Paulo city, between 19:35 GMT and 20:00 GMT the system reaches its maximum reflectivity in the city center and after that, it starts to decay, moving to southwest. This storm caused urban flooding which impaired the traffic in roads and subway lines. Its heavy rain and strong winds were responsible for closing MASP's airports (as observed by São Paulo civil defense, http://www.defesacivil.sp.gov.br/) and there were reports of hail in some neighborhoods.

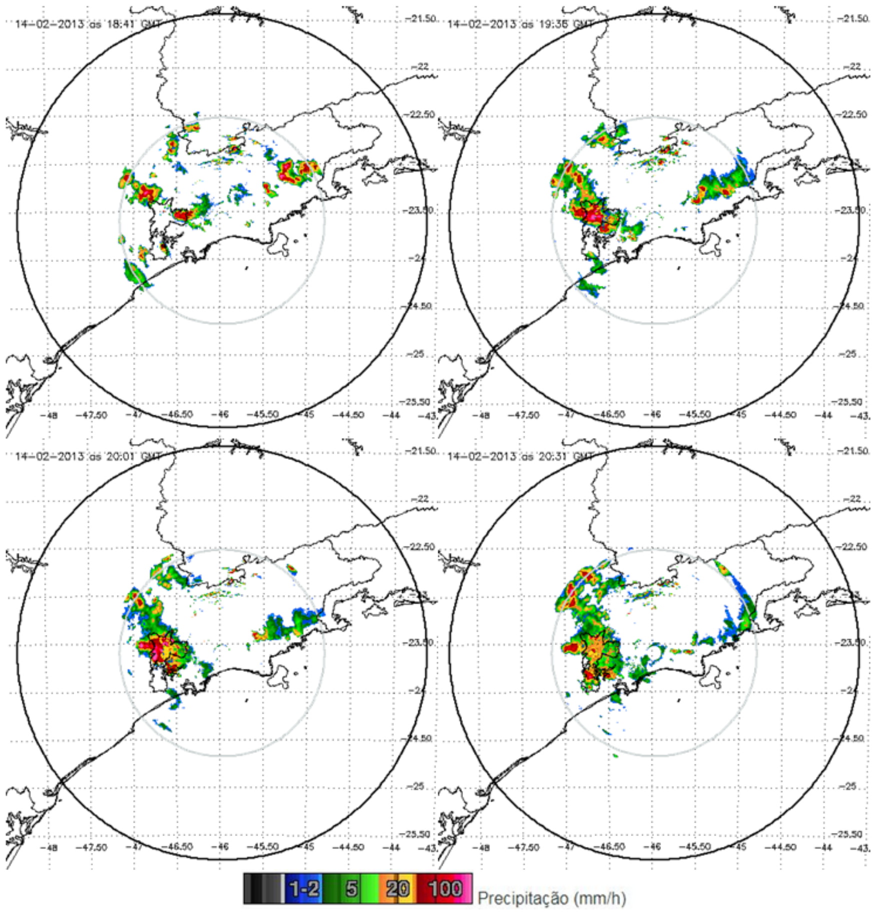

Fig 3 Reflectivity on CAPPI3km of Salesópolis radar. Fonte: http://radar.iag.usp.br

This was an interesting intense weather event in the metropolitan area, since it was an isolated convective cell that intensify as it moves toward the urban area. Fig 4 and Fig 5 compare observed and simulated accumulated precipitation. In the observations, we found accumulated values of 101 mm and 84 mm observed in less than 2 hours, as informed by the São Paulo state flood warning system (SAISP, *"Sistema de Alerta a Inundações do Estado de São Paulo"*) rain gauges. The control experiment, correspondent to Experiment 1 in table 1, succeeds to obtain a maximum peak close to the observed, although it was lightly displaced. If we compare all the stations, there is a little tendency for rain underestimation on the control experiment, which is acceptable, given the high variability of the observed precipitation in a such short space.

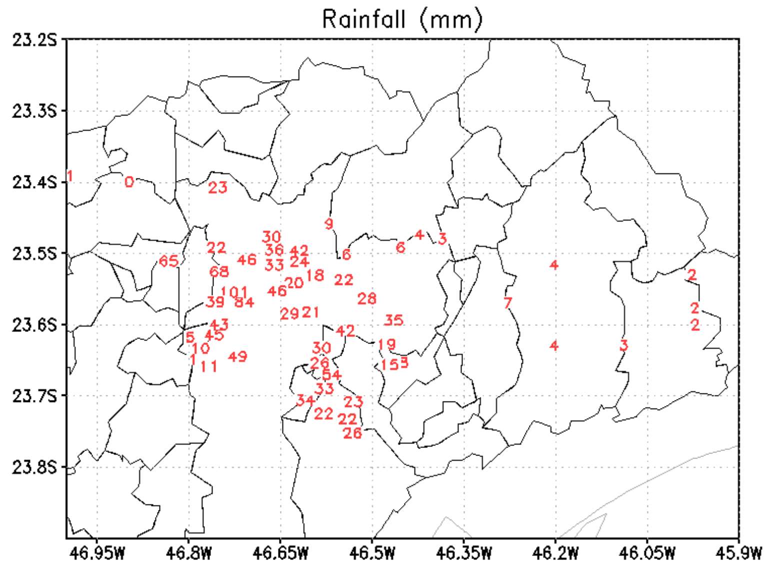

Fig 4 Accumulated rainfall (mm) during the event of February 14th, 2013, from SAISP (https://www.saisp.br/) and INMET (www.inmet.gov.br/) rain gauge stations.

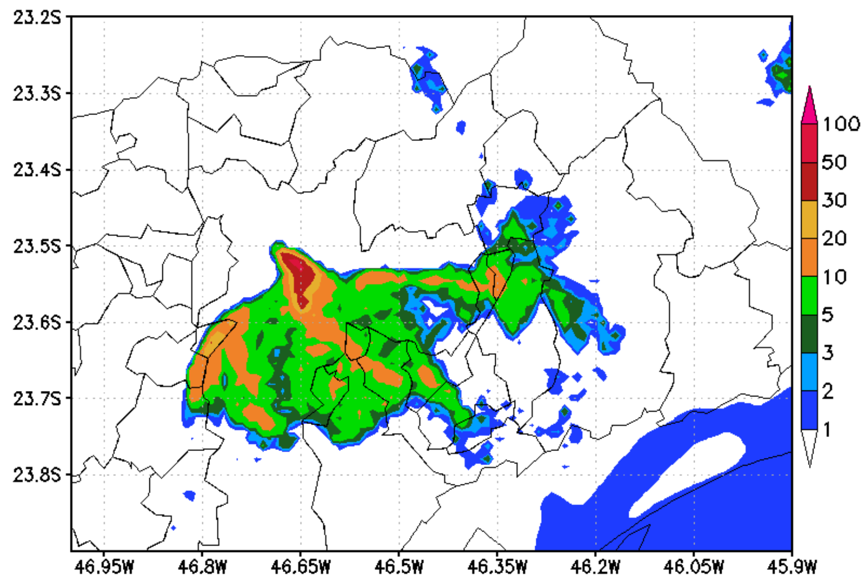

Fig 5 Precipitation accumulated (mm) during the event of February 14th, 2013, from Control Experiment (Experiment 1 in table 1).

The synoptic condition during this event was characterized, in low levels of the atmosphere, by a low-pressure center on northern Argentina and Paraguay, forcing moist and heat convergence since western Amazonia, where it is channelized by the Andes, until the Southern Brazil. After that, circulation went to a frontal zone located on South Atlantic, which also contributed to the moisture flow. In high levels, a diffluent area on

Brazilian side and a short-wave trough on northern Argentina, provided a weak support with cyclonic vorticity advection to the MASP. However, the surface South Atlantic Subtropical High (SASH) still keeping an anticyclonic circulation over São Paulo State. Temperatures were high and there was contribution of warm and moist advection coming from the ocean and northeastern Brazil. This configures a pre-frontal synoptic pattern over the MASP, with winds from northwest.

Fig 6 shows a comparison between the Campo de Marte – SP atmospheric sounding and a profile extracted from the Control Experiment run near to the launching location. There was a large variation on sounding's mid-level dew point, which was not well represented by the simulation, which presented a moister profile in general. For temperature, the experiment represents the sounding's average behavior, but it is almost 1 ºC warmer on the surface. Simulated wind profile is mainly from west and lightly underestimates the observation in intensity.

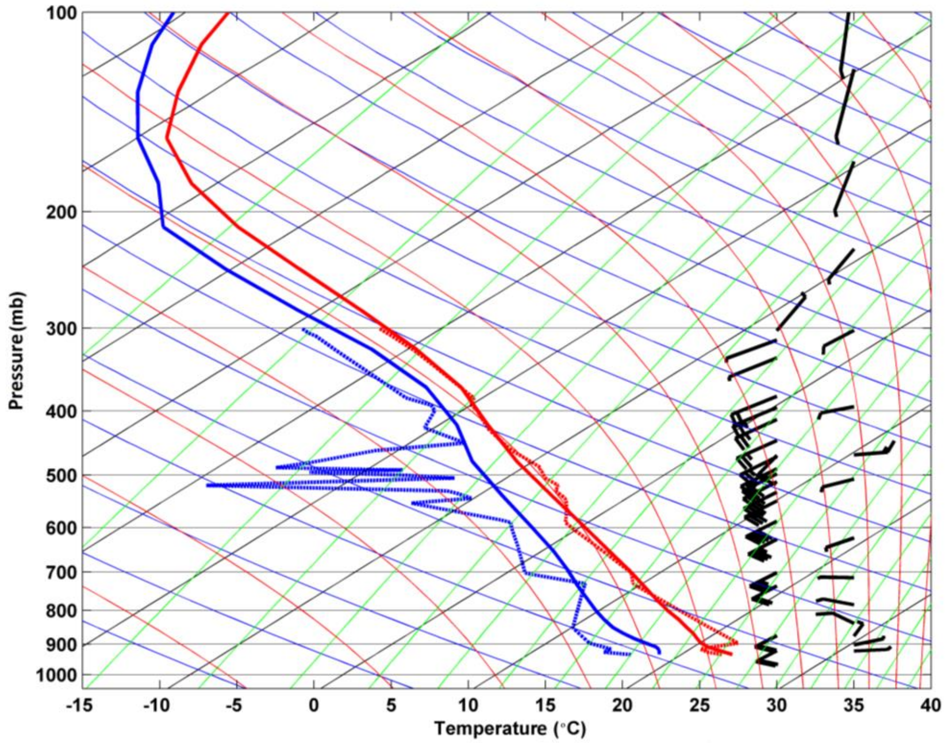

Fig 6 Sounding of Campo de Marte – SP (wind barbs on the left and dashed lines) and profile for the same lat/lon from Experiment 1 (wind barbs on the right and full lines). Temperature (ºC, red color) and Dew point (ºC, blue color).

We calculated convective parameters for the sounding and the Control Experiment profiles. A Convective Available Potential Energy, CAPE (Moncrieff and Miller, [1976], with the air parcel ascended from surface has 797 J kg^{-1} for the sounding and 2418 J kg^{-1} for the experiment. As explained for instability, CAPE is very sensitive with surface differences and, therefore, a warmer temperature and a moister dew point in the surface causes a higher CAPE in the experiment run. It also underestimates the Convective Inhibition (CIN) that has a value of -120 J kg^{-1} for the sounding and none for the experiment. It is important to notice that the experiment could not dry enough and it affects the instability parameters. Bulk Richardson Number (BRN) shear, defined as the magnitude of the difference between the 0-6-km density-weighted mean wind and the density-weighted mean wind of the lowest 0.5 km [*Evans and Doswell*, 2001], has a 16.9 m^2 s^{-2} for the sounding and 10.7 for the experiment. Storm-Relative Helicity performed for the first 3 km of atmosphere (SRH), as defined by Rasmussen and Blanchard [1998], has -50.7 m^2 s^{-2} for the sounding and -31.5 m^2 s^{-2} for the experiment. Differences in BRN shear and SRH can be explained because sounding has stronger winds around 450 mb (≈ 6 km), the same occurs close to 700 mb (≈ 3 km), this must cause a higher shear and elevate these parameters in the sounding.

CAPE and Lifted Index (LI) based on the air parcel ascended from surface [*Galway*, 1956] are plotted before the storm is generated (figure not shown), in an environment similar to the proximity soundings [*Brooks et al.*, 1994; *Brooks et al.*, 2003]. There is a very unstable area in the center of MASP, following the sea breeze front and where it reaches the central area with the hottest temperatures. Those high temperatures induce local low pressure and generate convergence over the central area, which accelerate the sea breeze front until it reaches the center of the urban region [*E D Freitas et al.*, 2007; *Khan and Simpson*, 2001]. We found CAPE values as high as 4000 J kg^{-1} and a LI values of -7.5 ºC, which is a thermodynamic profile favorable to the development of severe storm, including possible supercell, such as the sounding found by Nascimento [2004] from western Paraná (Brazil State), that also had large values of supercell composite parameter (SUP) and energy-helicity index (EHI). CIN was observed and reach minimum values of -10 J kg^{-1}, showing low inhibition to convection.

BRN shear and SRH (figure not show), which represent the amount of shear in the first 6 km of the atmosphere and the helicity (directional shear) in the first 3 km of atmosphere, respectively, is present following the sea breeze front. Close to MASP center, BRN shear reaches 30 m^2s^{-2}, above the threshold of 20 m^2s^{-2}, observed in severe weather environments (tornadic or not, Nascimento 2004). Thus, beside intense in thermodynamics, the event fast grew upscale maintain itself longer than an isolated cell. SRH reaches -50 m^2s^{-2}, which is weak when compared to the threshold of -150 m^2s^{-2} that favour tornadic supercells [*Mills and Colquhoun*, 1998].

4 Sensitivity Experiments with Future Urban Growth

4.1 Current building height in 2030's area

Fig 7 shows precipitation accumulated (mm) during the event of February 14th, 2013, for Experiment 2 that increase the area expansion, but keeps constant the buildings height. Comparing with current scenario (Experiment 1), in Fig 5, the wider urban area also has a precipitation spread in a larger area, which enhance the precipitation volume over MASP. This result is in agreement with those found by other authors who tested the urban land use impacts around the world, like in Carrió et al. [2010], Rozoff et al. [2003], Pathirana et al. [2014]; Mölders and Olson [2004], Zhong and Yang [2015], Souza et al [2016] and Freitas et al. [2009a].

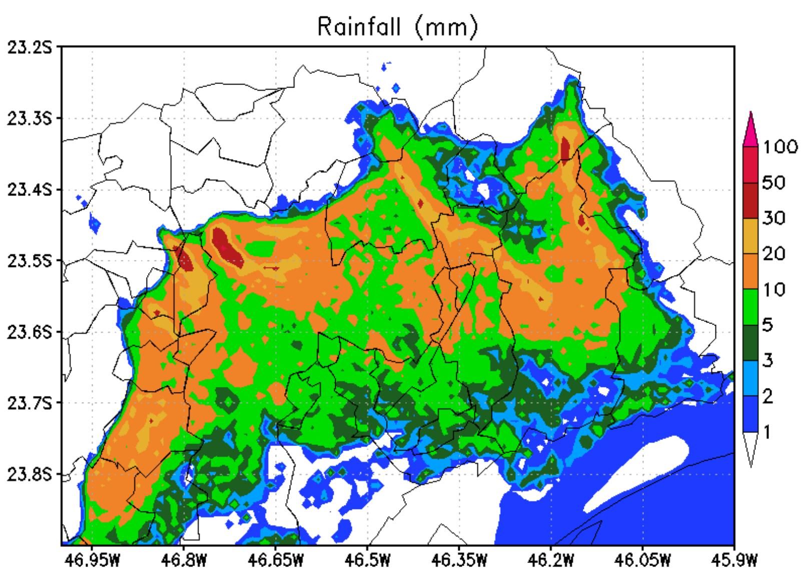

Fig 7 Accumulated precipitation (mm) during the event of February 14th, 2013, for Experiment 2.

There is a huge increase in the amount of precipitation taking the difference between the Experiment 2 and Experiment 1. On Experiment 2, temperature near to the surface (not shown) increases on places where land use changes to urban type. Thus, the sea breeze front reaches these places earlier, especially on east side of MASP, and drops the air temperature where it passes through. Wind at 10 m (not shown), had it magnitude increased.

4.2 Future building height in the current area

Fig 8 shows accumulated precipitation (mm) during the event of February 14th, 2013, for Experiment 3 that maintains the area, but change the height of the buildings. Experiment 3 decreases the amount of rainfall, including the maximum in more than 20 mm, compared with Experiment 1. Although there is not big differences between these experiment results, as we saw in Experiment 2.

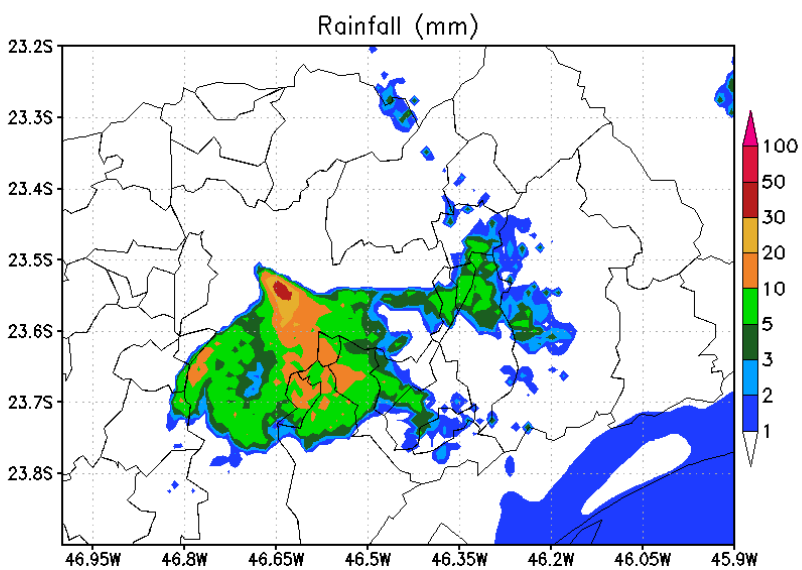

Fig 8 Accumulated precipitation (mm) during the event of February 14th, 2013, for Experiment 3.

Taking the difference between the Experiment 3 and Experiment 1, we see a very similar result for temperature, except on city center, where Experiment 3 has the maximum temperature near to the surface (not shown) decreased. Also, there is an area with increased temperatures, due to the blockade of the sea breeze front, indicating that it does not reach as far as in Experiment 1. 10 m height wind has a decreased intensity on central city due to the roughness in the area.

4.3 Future building height in 2030's area

Fig 9 shows accumulated precipitation (mm) during the event of February 14th, 2013, for Experiment 4. Comparing with Experiment 1 this scenario presents precipitation in a larger area, increasing precipitated volume over MASP. There is a rising in temperature on regions with new urban land use. On east side of MASP, the sea breeze front reaches the MASP center earlier. 10 m height wind has its intensity decreased due to higher roughness. Experiment 4 decreases the amount of rainfall compared to Experiment 2. There is an increase in temperature, which indicates the sea breeze did not reach the same place in Experiment 2. 10 m wind decreased intensity over all RMSP, except in the center, due to building roughness.

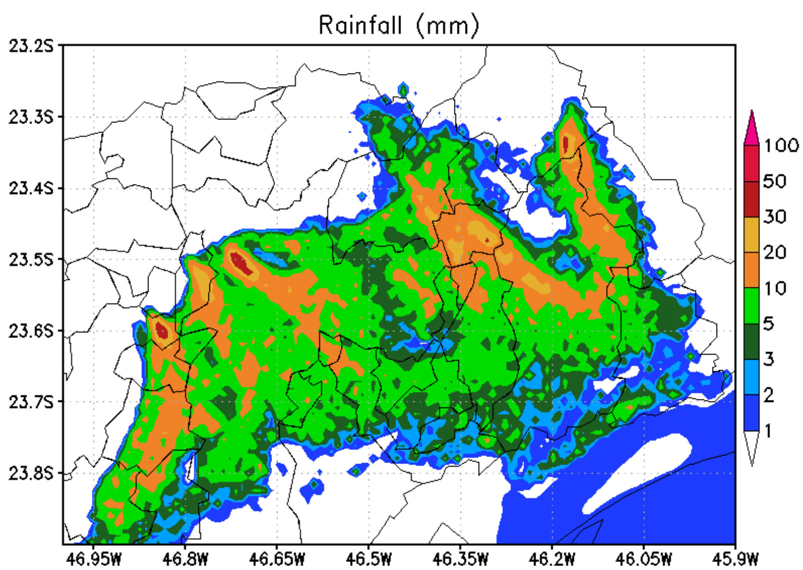

Fig 9 Accumulated precipitation (mm) during the event of February 14th, 2013, for Experiment 4.

4.4 Application of Factorial Planning/Factor Separation Method

Fig 10 shows the contribution of the urban area growth to the accumulated precipitation on 14th February, 2013, while Fig 11 shows the contribution of high-buildings area growth and Fig 12 the interaction between these two factors. We see that urban area growth is capable to increase the amount of precipitation over new urban areas. In areas with old urban use, it is not clear, but there is a weak tendency of rainfall increasing. It shows that the change in urban use from rural to urban is determinant to rainfall increase. The rainfall induced by high-building area growth shows a decrease in precipitation, also confines it to southern areas. The interaction between these factors shows a behavior between this two factors, it increases the amount of precipitation but less and southern than UAE.

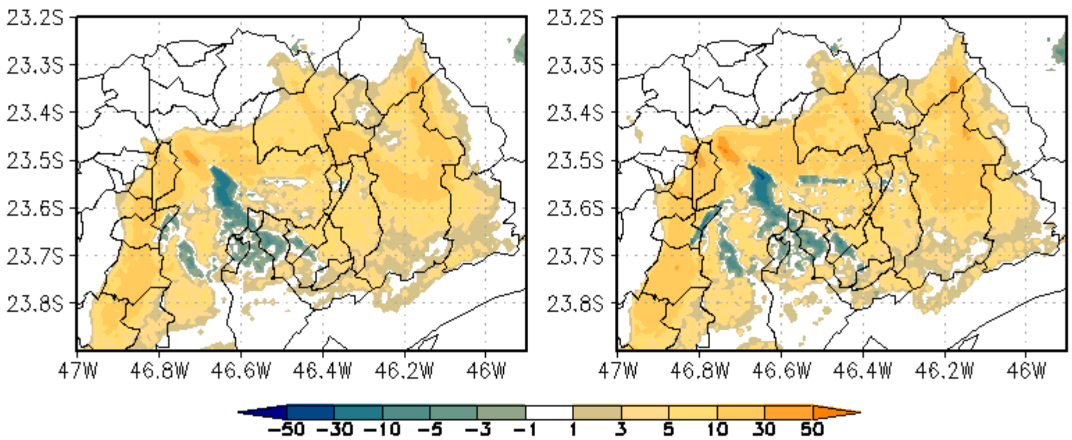

Fig 10 Precipitation induced by urban area growth (UAE). Factorial Planning (left) and Factor Separation (right).

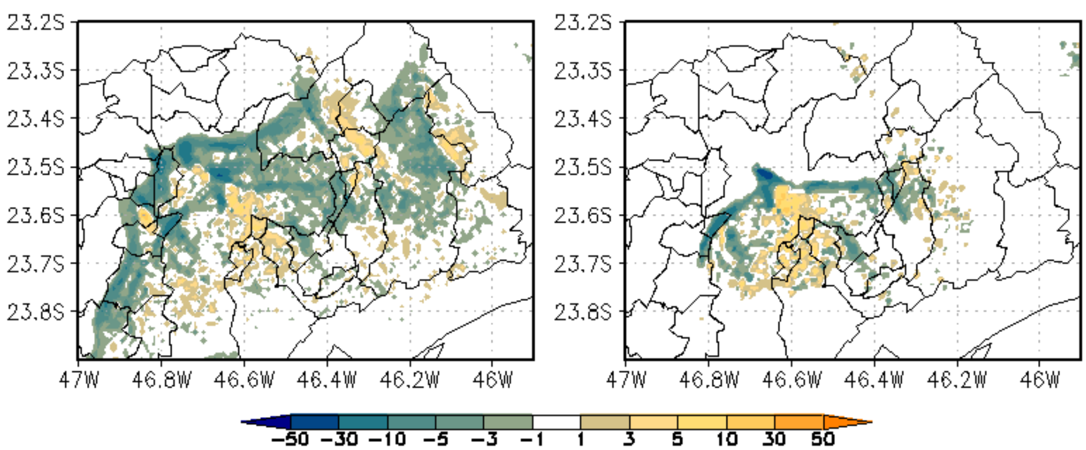

Fig 11 Precipitation induced by high-building area growth (HBAE). Factorial Planning (left) and Factor Separation (right).

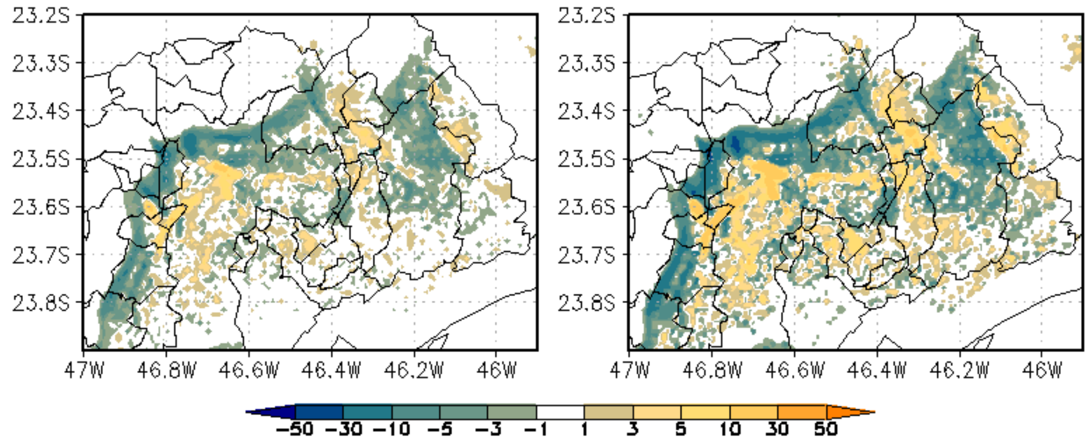

Fig 12 Precipitation induced by the interaction between urban area growth and high-building area growth (UAE_HBAE). Factorial Planning (left) and Factor Separation (right).

Fig 13 shows CAPE induced by urban area growth, while Fig 14 shows CAPE induced by high-buildings area growth and Fig 15 shows the interaction between these two factors. We see that both factors and its interaction contribute to increase CAPE. Although, the building barrier affects the sea breeze front, which brings more instability to the MASP. This drops CAPE on places it could be higher.

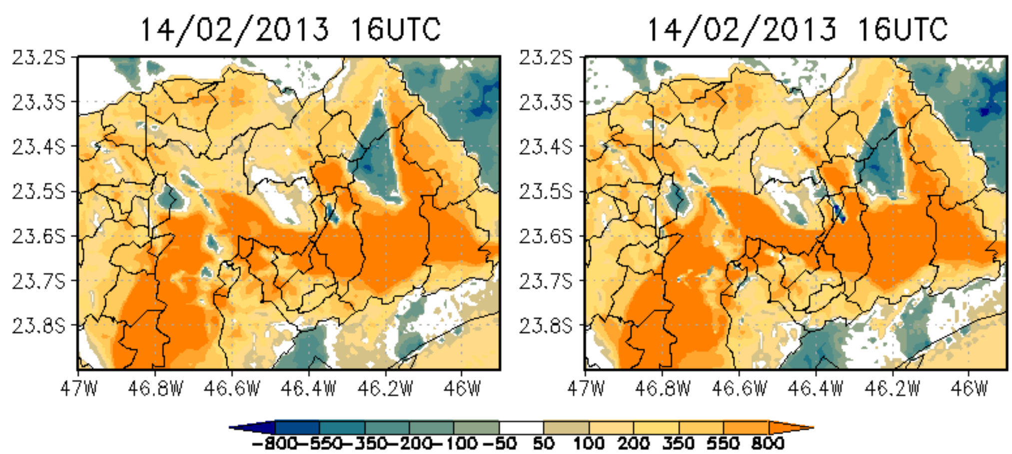

Fig 13 CAPE induced by urban area growth (UAE). Factorial Planning (left) and Factor Separation (right).

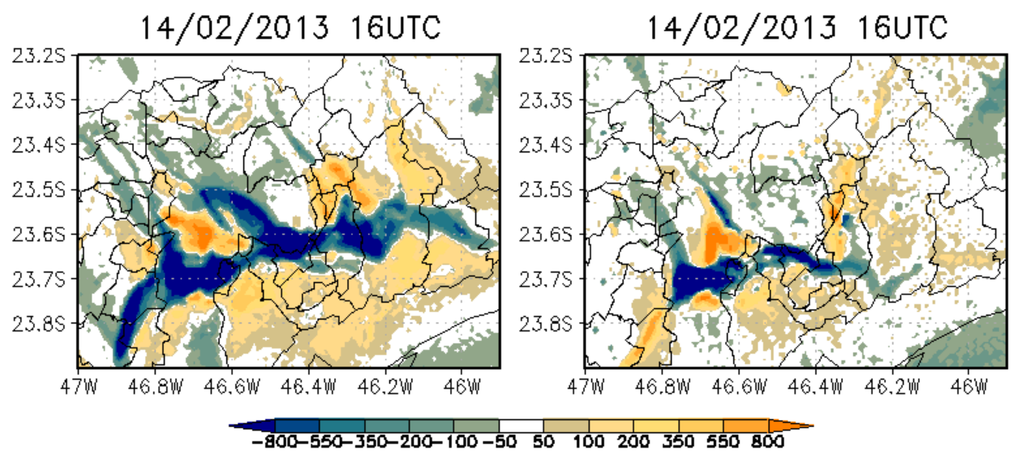

Fig 14 CAPE induced by high-building area growth (HBAE). Factorial Planning (left) and Factor Separation (right).

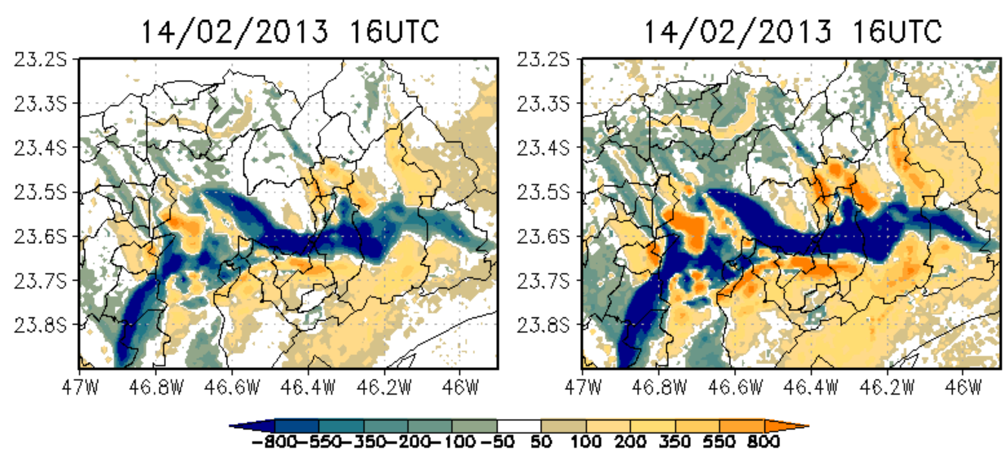

Fig 15 CAPE induced by the interaction between urban area growth and high building area growth (UAE_HBAE). Factorial Planning (left) and Factor Separation (right).

LI induced by urban area growth (figure not shown) has again a raise in instability with smaller values, all over new urban area. LI induced by high-buildings area growth (figure not shown) increased LI where sea breeze front does not reach. The interaction between these two factors (figure not shown) also shows the same.

BRN shear induced by urban area growth (Fig 16) has a tendency to increase in MASP. The sea breeze front it is a source of shear, due to its circulation. Therefore, HBAE decreases shear on MASP centre, where it blocks the front. The interaction between these two factors shows an increase in shear due to UAE and a decrease on sea breeze front blockade.

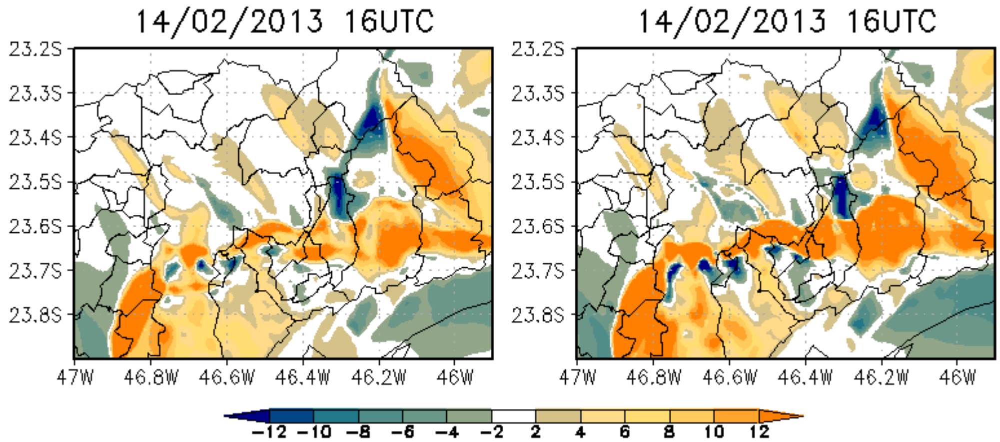

Fig 16 BRN shear induced by urban area growth (UAE). Factorial Planning (left) and Factor Separation (right).

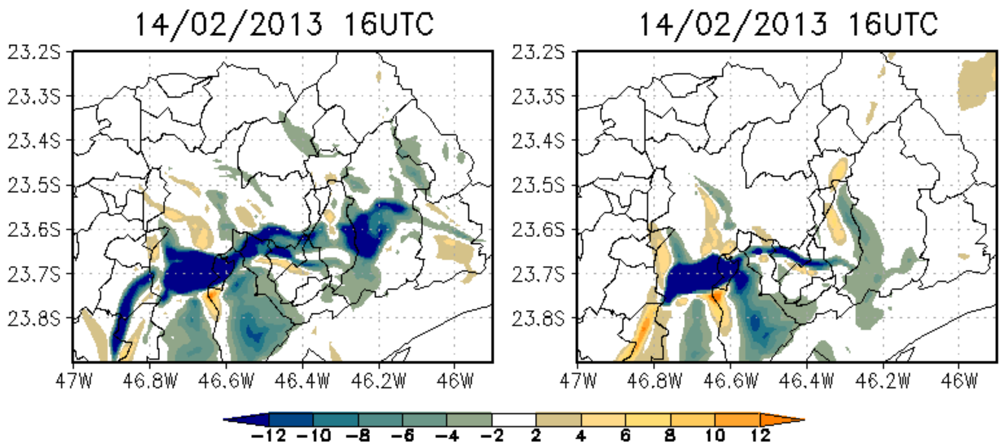

Fig 17 BRN shear induced by high-building area growth (HBAE). Factorial Planning (left) and Factor Separation (right).

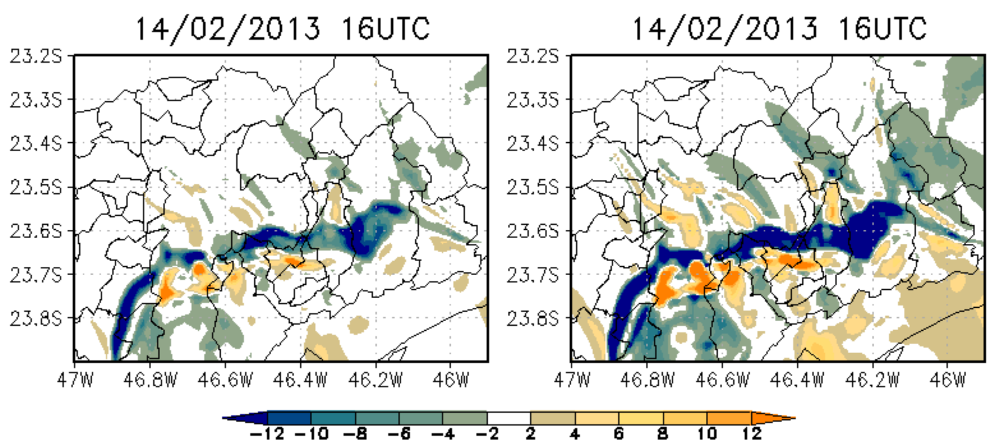

Fig 18 BRN shear induced by the interaction between urban area growth and high building area growth (UAE_HBAE). Factorial Planning (left) and Factor Separation (right).

6 Conclusions

In the environment just before the storm, extremely unstable profiles were obtained, with some degree of organization and low probability of tornadic supercells, as expected for this storm case.

The factorial planning and factor separation methods show that 2030's urban area is capable to increase the amount of precipitation over MASP. It indicates that change rural to urban land use is determinant for this increase. On the other hand, the high-building area growth brings a tendency for precipitation supress. The interaction between these factors show a behaviour in the middle of these two effects, it increases area with precipitation less than could be in an urban soil with low buildings.

Both factors generate instability due to its sources of latent and sensible heat and the building barrier blocks the source of instability and shear that sea breeze front brings. Then, the interaction of the factors favours severity on southern places.

Acknowledgments

This study was financed in part by the Coordenação de Aperfeiçoamento de Pessoal de Nível Superior - Brasil (CAPES) - Finance Code 001. The first author also acknowledge the National Council for Scientific and Technological Development – CNPq – for her scholarship. We also acknowledge the São Paulo Research Foundation for the financial support this study (Process number 2015/14497-0).

References

Barros Neto, B., I. S. Scarmino, and R. E. Bruns (1995), *Planejamento e otimização de experimentos*, Segunda Edição ed., Campinas.

Brooks, H. E., C. A. Doswell, and J. Cooper (1994), On the Environments of Tornadic and Nontornadic Mesocyclones, *Weather and Forecasting*, *9*(4), 606-618, doi:10.1175/1520-0434(1994)009<0606:OTEOTA>2.0.CO;2.

Brooks, H. E., J. W. Lee, and J. P. Craven (2003), The spatial distribution of severe thunderstorm and tornado environments from global reanalysis data, *Atmospheric Research*, *67-68*, 73-94, doi:https://doi.org/10.1016/S0169-8095(03)00045-0.

Carraça, M. G. D., and C. G. Collier (2007), Modelling the impact of high-rise buildings in urban areas on precipitation initiation, *Meteorological Applications*, *14*(2), 149-161, doi:10.1002/met.15.

Carrió, G. G., W. R. Cotton, and W. Y. Y. Cheng (2010), Urban growth and aerosol effects on convection over Houston: Part I: The August 2000 case, *Atmospheric Research*, *96*(4), 560-574, doi:https://doi.org/10.1016/j.atmosres.2010.01.005.

Chen, C., and W. R. Cotton (1983), A one-dimensional simulation of the stratocumulus-capped mixed layer, *Boundary-Layer Meteorology*, *25*(3), 289-321.

Cotton, W. R., and R. A. Anthes (1992), *Storm and Cloud Dynamics*, 1st Edition ed., Academic Press.

Cotton, W. R., and R. A. Pielke (1995), *Human Impacts on Weather and Climate*, 288 pp., Cambridge University Press.

Evans, J. S., and C. A. Doswell (2001), Examination of Derecho Environments Using Proximity Soundings, *Weather and Forecasting*, *16*(3), 329-342, doi:10.1175/1520-0434(2001)016<0329:EODEUP>2.0.CO;2.

Freitas, E. D., C. M. Rozoff, W. R. Cotton, and P. L. S. Dias (2007), Interactions of an urban heat island and sea-breeze circulations during winter over the metropolitan area of Sao Paulo, Brazil, *Boundary-Layer Meteorology*, *122*(1), 43-65, doi:10.1007/s10546-006-9091-3.

Freitas, E. D., P. L. Silva Dias, V. S. B. Carvalho, C. R. Mazzoli, L. D. Martins, J. A. Martins, and M. F. Andrade (2009a), Factors involved in the formation and development of severe weather conditions over the Megacity of São Paulo, in *89th American Meteorological Society Meeting*, edited, AMS, Phoenix, AZ.

Freitas, S. R., et al. (2009b), The coupled aerosol and tracer transport model to the Brazilian developments on the regional atmospheric modeling system (CATT-BRAMS) Part 1: model description and evaluation, *Atmospheric Chemistry and Physics*, *9*, 2843-2861, doi:10.5194/acp-9-2843-2009.

Freitas, S. R., K. M. Longo, M. A. F. Silva Dias, P. L. Silva Dias, R. Chatfield, E. Prins, P. Artaxo, G. A. Grell, and F. S. Recuero (2005), Monitoring the transport of biomass burning emissions in South America, *Environmental Fluid Mechanics*, *5*(1-2), 135-167, doi:10.1007/s10652-005-0243-7.

Galway, J. G. (1956), The Lifted Index as a Predictor of Latent Instability, *Bulletin of the American Meteorological Society*, *37*(10), 528-529, doi:10.1175/1520-0477-37.10.528.

Grell, G. A., and D. Devenyi (2002), A generalized approach to parameterizing convection combining ensemble and data assimilation techniques, *Geophysical Research Letters*, *29*(14), 38-31–38-34, doi:10.1029/2002GL015311.

Grimmond, C. and Oke, T. (1999) Aerodynamic properties of urban areas derived from analysis of surface form. *Journal of Applied Meteorology and Climatology*, 38, 1262–1292.

Haddad, E. A., and E. Teixeira (2015), Economic impacts of natural disasters in megacities: The case of floods in São Paulo, Brazil, *Habitat International*, *45, Part 2*, 106-113, doi:http://dx.doi.org/10.1016/j.habitatint.2014.06.023.

Han, J., J. Baik, and A. P. Khain (2012), A Numerical Study of Urban Aerosol Impacts on Clouds and Precipitation, *Journal of the Atmospheric Sciences*, *69*(2), 504-520, doi:10.1175/JAS-D-11-071.1.

Johns, R. H., and C. A. Doswell (1992), Severe Local Storms Forecasting, *Weather and Forecasting*, *7*(4), 588-612, doi:10.1175/1520-0434(1992)007<0588:SLSF>2.0.CO;2.

Karam, H. A., A. J. Pereira Filho, V. Masson, J. Noilhan, and E. P. Marques Filho (2010), Formulation of a tropical town energy budget (t-TEB) scheme, *Theoretical and Applied Climatology*, *101*(1-2), 109-120, doi:10.1007/s00704-009-0206-x.

Kaufmann, R. K., K. C. Seto, A. Schneider, Z. Liu, L. Zhou, and W. Wang (2007), Climate Response to Rapid Urban Growth: Evidence of a Human-Induced Precipitation Deficit, *Journal of Climate*, *20*(10), 2299-2306, doi:10.1175/JCLI4109.1.

Khan, S., and R. Simpson (2001), Effect of a heat island on the meteorology of a complex urban airshed, *Boundary-Layer Meteorology*, *100*(3), 487-506, doi:10.1023/A:1019284332306.

Kusaka, H., K. Nawata, A. Suzuki-Parker, Y. Takane, and N. Furuhashi (2014), Mechanism of Precipitation Increase with Urbanization in Tokyo as Revealed by Ensemble Climate Simulations, *Journal of Applied Meteorology and Climatology*, *53*(4), 824-839, doi:10.1175/JAMC-D-13-065.1.

Masson, V. (2000), A physically-based scheme for the urban energy budget in atmospheric models, *Boundary-Layer Meteorology*, *94*(3), 357-397, doi:10.1023/A:1002463829265.

Mellor, G. L., and T. Yamada (1982), Development of a turbulence closure-model for geophysical fluid problems, *Reviews of Geophysics*, *20*(4), 851-875, doi:10.1029/RG020i004p00851.

Meyers, M. P., R. L. Walko, J. Y. Harrington, and W. R. Cotton (1997), New RAMS cloud microphysics parameterization. Part II: The two-moment scheme, *Atmospheric Research*, *45*(1), 3-39, doi:http://dx.doi.org/10.1016/S0169-8095(97)00018-5.

Mills, G. A., and J. R. Colquhoun (1998), Objective Prediction of Severe Thunderstorm Environments: Preliminary Results Linking a Decision Tree with an Operational Regional NWP Model, *Weather and Forecasting*, *13*(4), 1078-1092, doi:10.1175/1520-0434(1998)013<1078:OPOSTE>2.0.CO;2.

Moller, A. R. (2001), Severe Local Storms Forecasting, in *Severe Convective Storms*, edited by C. A. Doswell, pp. 433-480, American Meteorological Society, Boston, MA, doi:10.1007/978-1-935704-06-5_11.

Moncrieff, M. W., and M. J. Miller (1976), The dynamics and simulation of tropical cumulonimbus and squall lines, *Quarterly Journal of the Royal Meteorological Society*, *102*(432), 373-394, doi:10.1002/qj.49710243208.

Morales, C. A., R. P. da Rocha, and R. Bombardi (2010), On the development of summer thunderstorms in the city of São Paulo: Mean meteorological characteristics and pollution effect, *Atmospheric Research*, *96*(2), 477-488, doi:https://doi.org/10.1016/j.atmosres.2010.02.007.

Mölders, N., and M. A. Olson (2004), Impact of Urban Effects on Precipitation in High Latitudes, *Journal of Hydrometeorology*, *5*(3), 409-429, doi:10.1175/1525-7541(2004)005<0409:IOUEOP>2.0.CO;2.

Nascimento, E. (2004), Identifying Severe Thunderstorm Environments in Southern Brazil: Analysis of Severe Weather Parameters, paper presented at 22nd

Conference on Severe Local Storms, American Meteorological Society, Hyannis, MA, EUA.

Pathirana, A., H. B. Denekew, W. Veerbeek, C. Zevenbergen, and A. T. Banda (2014), Impact of urban growth-driven landuse change on microclimate and extreme precipitation — A sensitivity study, *Atmospheric Research*, *138*, 59-72, doi:https://doi.org/10.1016/j.atmosres.2013.10.005.

Rasmussen, E. N., and D. O. Blanchard (1998), A Baseline Climatology of Sounding-Derived Supercell andTornado Forecast Parameters, *Weather and Forecasting*, *13*(4), 1148-1164, doi:10.1175/1520-0434(1998)013<1148:ABCOSD>2.0.CO;2.

Rojas, J. L. F., A. J. Pereira Filho, H. A. Karam, F. Vemado, and V. Masson (2018), Effects of Explicit Urban-Canopy Representation on Local Circulations Above a Tropical Mega-City, *Boundary-Layer Meteorology*, *166*(1), 83-111, doi:10.1007/s10546-017-0292-8.

Rosenfeld, D. (2000), Suppression of Rain and Snow by Urban and Industrial Air Pollution, *Science*, *287*(5459), 1793.

Rozoff, C. M., W. R. Cotton, and J. O. Adegoke (2003), Simulation of St. Louis, Missouri, Land Use Impacts on Thunderstorms, *Journal of Applied Meteorology*, *42*(6), 716-738, doi:10.1175/1520-0450(2003)042<0716:SOSLML>2.0.CO;2.

Silva Dias, M. A. F., J. Dias, L. M. V. Carvalho, E. D. Freitas, and P. L. Silva Dias (2013), Changes in extreme daily rainfall for São Paulo, Brazil, *Climatic Change*, *116*(3-4), 705-722, doi:10.1007/s10584-012-0504-7.

Souza, D. O., R. C. S. Alvalá, and M. G. Nascimento (2016), Urbanization effects on the microclimate of Manaus: A modeling study, *Atmospheric Research*, *167*, 237-248, doi:https://doi.org/10.1016/j.atmosres.2015.08.016.

Stein, U., and P. Alpert (1993), Factor Separation in Numerical Simulations, *Journal of the Atmospheric Sciences*, *50*(14), 2107-2115, doi:10.1175/1520-0469(1993)050<2107:FSINS>2.0.CO;2.

Tarifa, J. and Azevedo, T. (2001) Os climas na cidade de São Paulo: teoria e prática, primeira edn. GEOUSP, Coleção Novos Caminhos.

Thompson, R. L., R. Edwards, J. A. Hart, K. L. Elmore, and P. Markowski (2003), Close Proximity Soundings within Supercell Environments Obtained from the Rapid Update Cycle, *Weather and Forecasting*, *18*(6), 1243-1261, doi:10.1175/1520-0434(2003)018<1243:CPSWSE>2.0.CO;2.

van den Heever, S. C., and W. R. Cotton (2007), Urban Aerosol Impacts on Downwind Convective Storms, *Journal of Applied Meteorology and Climatology*, *46*(6), 828-850, doi:10.1175/JAM2492.1.

Villaça, F. J. M. (1978) The territorial structure of the Brazilian Southern megacity (A estrutura territorial da metrópole sul brasileira). Ph. D. Thesis. FFLCH/USP, Departamento de Geografia. (in Portuguese)

Walko, R. L., W. R. Cotton, M. P. Meyers, and J. Y. Harrington (1995), New RAMS cloud microphysics parameterization Part I: the single-moment scheme, *Atmospheric Research*, *38*(1), 29-62, doi:10.1016/0169-8095(94)00087-T.

Wieringa, J. (1993) Representative Roughness Parameters for Homogeneous Terrain, *Boundary-Layer Meteorology*, 63, 323–363.

Xue, M., K. K. Droegemeier, and V. Wong (2000), The Advanced Regional Prediction System (ARPS) – A multi-scale nonhydrostatic atmospheric simulation and prediction model. Part I: Model dynamics and verification, *Meteorology and Atmospheric Physics*, *75*(3), 161-193, doi:10.1007/s007030070003.

Young, A. F. (2013), Urban expansion and environmental risk in the São Paulo Metropolitan Area, *Climate Research*, *57*(1), 73-80.

Zhong, S., and X. Yang (2015), Ensemble simulations of the urban effect on a summer rainfall event in the Great Beijing Metropolitan Area, *Atmospheric Research*, *153*, 318-334, doi:https://doi.org/10.1016/j.atmosres.2014.09.005.